

Forum

One-Dimensional Colloidal Gold and Silver Nanostructures

Catherine J. Murphy,* Anand M. Gole, Simona E. Hunyadi, and Christopher J. Orendorff

Department of Chemistry and Biochemistry, University of South Carolina, 631 Sumter Street, Columbia, South Carolina 29208

Received November 9, 2005

One-dimensional (1-D) metallic nanoscale materials have long been of interest to many groups of scientists. Within the last 2 decades, great advances in the synthesis of metallic nanorods and nanowires have been made, with a variety of templating methods. More recently, bottom-up chemical syntheses of these materials have become increasingly reported in the literature. This Forum Article describes the synthesis, physical properties, and potential applications of 1-D metals, with an emphasis on silver and gold derived from studies in the authors' laboratories.

I. Introduction

Inorganic nanoparticles are inorganic materials in which the particle diameter is in the ~ 1 –100-nm regime. Although the scientific literature has produced a staggering amount of experiment and theory on these materials in all three basic electronic categories of inorganic substances—metals, semiconductors, and insulators—since the 1990s, in this Forum Article we focus exclusively on metals, in particular, gold and silver. Gold and silver strongly absorb and scatter light in the visible region of the electromagnetic (EM) spectrum and are stable to oxidation, compared to other metals; these two properties in large part account for their popularity in the inorganic nanomaterials community. In addition to reviewing some of the extensive literature in this area, we highlight some recent results from our own laboratory and include new results on the surface functionalization of gold and silver nanorods/nanowires.

The use of metals by humans, of course, dates back thousands of years, yet humans have been using metal nanoparticles for only hundreds of years. For example, stained glass windows from the late 1400s and later can contain gold, which, when “finely divided”, gives the glass a beautiful red color that can stand centuries of sunlight without fading.^{1,2} Brilliant Medieval and Renaissance pottery

glazes attain their color, at least in part, to the presence of copper and silver nanoparticles.³ Faraday prepared brightly colored colloidal gold nanoparticle solutions in the mid-1850s that are still on display today in the Royal Institution's Faraday Museum in London. In these examples, the metal nanoparticles have optical properties different from the bulk.^{4–6} As many others have pointed out,^{4–6} Gustav Mie in 1908 published a seminal paper⁷ in which the optical properties of metal spheres were explained by the solutions to Maxwell's equations under the appropriate conditions. In essence, upon incident EM radiation of a given wavelength, the delocalized conduction-band electrons in a metal collectively oscillate to produce what is now generally called a “plasmon” band. Mie's paper has been cited over 1500 times since 1991, a tribute to the interest the scientific community has in the physical properties of metal nanoparticles.

* To whom correspondence should be addressed. E-mail: Murphy@mail.chem.sc.edu.

(1) Williamson, S. J.; Cummins, H. Z. *Light and Color in Nature and Art*; Wiley: New York, 1983.

- (2) Murphy, C. J. *Science* **2002**, *298*, 2139–2141.
 (3) Padovani, S.; Sada, C.; Mazzoldi, P.; Brunetti, B.; Borgia, I.; Sgamellotti, A.; Giulivi, A.; D'Acapito, F.; Battaglin, G. *J. Appl. Phys.* **2003**, *93*, 10058–10063.
 (4) El-Sayed, M. A. *Acc. Chem. Res.* **2001**, *34*, 257–264.
 (5) (a) Feldheim, D. L.; Foss, C. A., Jr. In *Metal Nanoparticles: Synthesis, Characterization, and Applications*; Feldheim, D. L., Foss, C. A., Jr., Eds.; Marcel Dekker: New York, 2002. (b) Kelly, K. L.; Jensen, T. R.; Lazarides, A. A.; Schatz, G. C. In *Metal Nanoparticles: Synthesis, Characterization, and Applications*; Feldheim, D. L., Foss, C. A., Jr., Eds.; Marcel Dekker: New York, 2002. (c) Kreibig, U.; Volmer, M. *Optical Properties of Small Metal Clusters*; Springer: Berlin, 1995. (d) Haes, A. J.; Stuart, D. A.; Nie, S.; Van Duyne, R. P. *J. Fluoresc.* **2004**, *14*, 355–367.
 (6) Lerme, J. *Eur. Phys. J. D* **2000**, *10*, 265–277.
 (7) Mie, G. *Ann. Phys.* **1908**, *25*, 377.

As interesting as spherical metal nanoparticles are, one-dimensional (1-D) metal nanostructures, in which the short axis of the material is in the ~ 1 –100-nm regime but the long axis is up to microns long, are of even more fundamental and practical interest in recent years.^{8–10} A recent issue of *Advanced Materials* [2003, 15 (5)], for example, was entirely devoted to 1-D nanostructures of all sorts and is a good companion to the present Forum Articles in this issue of *Inorganic Chemistry*. What are the reasons to become enamored of metal nanorods, nanowires, or 1-D chains of metal nanoparticles? From the viewpoint of fundamental physics, when the dimension of the metal particle is smaller than the mean free path of a conduction-band electron in a metal (\sim tens of nanometers), conductivity will decrease because the electrons are scattered by the surface, which in turn also implies that the magnitude of the effective optical constants is decreased.¹¹ For electrons confined in a long metallic nanowire, these confinement effects should occur along the diameter of the nanowire and, in theory, are well-understood; however, unusual collective excitation of spin and charge states within a 1-D conductor represents exciting frontiers in physics.¹² Nanoelectronic devices may require metallic nanowires to connect up to the macroworld, and any unusual effects need to be understood for device fabrication.⁹ Ferromagnetic metals such as nickel and cobalt, when physically confined to one dimension by virtue of being made in nanoporous membranes, show greatly enhanced magnetic properties.¹³ The mechanical properties of materials improve as they get smaller; for instance, the yield strength of gold nanowires increases as the diameter decreases.¹⁴ Anisotropic metal nanoparticles can absorb and scatter light along multiple axes; therefore, metal nanorods and nanowires have both longitudinal (along the long axis) and transverse (along the short axis) plasmon bands^{4,5,15} (Figure 1). EM energy can be guided coherently down chains of closely spaced metal nanoparticles because of near-field coupling of their plasmons;¹⁶ these discoveries support the notion that optical computing, and optical sensing, with metal nanoparticle arrays, is achievable.

Surface-enhanced spectroscopies, in which molecules near metal nanoparticle surfaces have larger signals than mol-

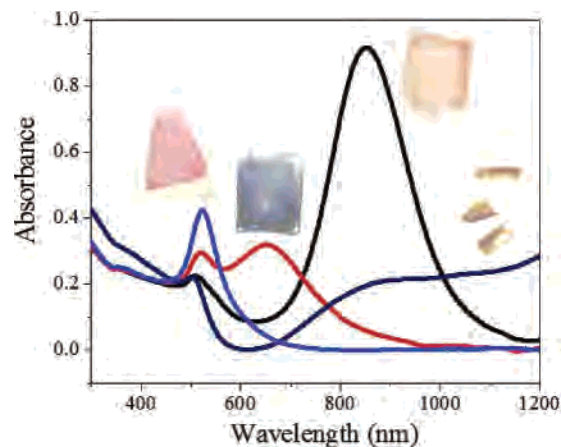


Figure 1. Absorption spectra of gold nanospheres (blue trace, 29 ± 5 nm diameter) and nanorods of aspect ratio 1.7 ± 0.2 (red trace, length = 41 ± 3 , width = 24 ± 3 nm), 4.5 ± 0.2 (black trace, length = 57 ± 8 , width = 13 ± 2 nm), and 16 ± 5 (navy trace, length = 372 ± 119 , width = 23 ± 4 nm). The corresponding inset pictures show the observed color of nanoparticles incorporated in transparent PVA from red (29 nm spheres) to tan (aspect ratio 16 rods).

ecules free in solution, are also exciting frontiers for chemistry and will be examined in more depth in the following.

Taken together, the literature suggests that 1D metallic nanostructures are highly interesting from multiple perspectives. (Also, this is still not taking into account unusual catalytic activities of gold on the nanoscale,¹⁷ which has not been explored for gold nanowires to our knowledge.) The questions inorganic chemists ask now are, “how do we make them, in high yield and high purity?” and “how can we manipulate them?” In the sections that follow, we principally describe our own approach in colloidal solution, but the reader is reminded that a great deal of excellent synthetic work in hard templates,¹⁸ against step edges of surfaces,^{19a} and in many forms of lithography^{19b} is also in progress for making 1-D metal nanostructures.

II. Synthesis and Mechanistic Studies of Colloidal Metallic Nanorods and Nanowires

II.A. Gold. Gold nanorods have been synthesized by a variety of methods.^{4,5,15} For this Forum Article, we will focus on the colloidal route, for which aspect ratios (length divided by width) of the materials can be controllably varied between

(8) Cao, G. *Nanostructures and Nanomaterials: Synthesis, Properties and Applications*; Imperial College Press: London, 2004.

(9) Hu, J.; Odom, T. W.; Lieber, C. M. *Acc. Chem. Res.* **1999**, *32*, 435–445.

(10) Xia, Y.; Yang, P.; Sun, Y.; Wu, Y.; Mayers, B.; Gates, B.; Yin, Y.; Kim, F.; Yan, H. *Adv. Mater.* **2003**, *15*, 353–389.

(11) Heavens, O. S. *Optical Properties of Thin Solid Films*; Dover: New York, 1991.

(12) (a) Fabrizio, M.; Gogolin, A. O. *Phys. Rev. B* **1995**, *51*, 17827–17842.

(b) Bockrath, M.; Cobden, D. H.; Lu, J.; Rinzler, A. L.; Smalley, R. E.; Balents, T.; McEuen, P. L. *Nature* **1999**, *397*, 598–601. (c) Segovia, P.; Purdie, D.; Hensberger, M.; Baer, Y. *Nature* **1999**, *402*, 504–507.

(13) Whitney, T. M.; Jiang, J. S.; Searson, P. C.; Chien, C. L. *Science* **1993**, *261*, 1316–1319.

(14) (a) Gall, K.; Diao, J.; Dunn, M. L. *Nano Lett.* **2004**, *4*, 2431–2436. (b) Gao, H. J.; Ji, B. H.; Jager, I. L.; Arzt, E.; Fratzl, P. *Proc. Natl. Acad. Sci. U.S.A.* **2003**, *100*, 5597–5600.

(15) (a) Daniel, M.-C.; Astruc, D. *Chem. Rev.* **2004**, *104*, 293–346. (b) Perez-Juste, J.; Pastoriza-Santos, J.; Liz-Marzan, L. M.; Mulvaney, P. *Coord. Chem. Rev.* **2005**, *249*, 1870–1901. (c) Murphy, C. J.; Sau, T. K.; Gole, A.; Orendorff, C. J.; Gao, J.; Gou, L.; Hunyadi, S.; Li, T. *J. Phys. Chem. B* **2005**, *109*, 13857–13870.

(16) (a) Maier, S. A.; Brongersma, M. L.; Kik, P. G.; Meltzer, S.; Requichia, A. A. G.; Atwater, H. *Adv. Mater.* **2001**, *13*, 1501–1505. (b) Maier, S. A.; Kik, P. G.; Atwater, H. A.; Meltzer, S.; Harel, E.; Koel, B. E.; Requichia, A. A. *Nat. Mater.* **2003**, *2*, 229–232. (c) Law, M.; Sibuly, D. J.; Johnson, J. C.; Goldberger, J.; Saykally, R. J.; Yang, P. *Science* **2004**, *305*, 1269–1273. (d) Wei, Q.-H.; Su, K.-H.; Durant, S.; Zhang, X. *Nano Lett.* **2004**, *4*, 1067–1071. (e) Lin, S.; Li, M.; Dujardin, E.; Mann, S. *Adv. Mater.* **2005**, *17*, 2553–2559.

(17) (a) Valden, M.; Lai, X.; Goodman, D. W. *Science* **1998**, *281*, 1647–1650. (b) Chen, M. S.; Goodman, D. W. *Science* **2004**, *306*, 252–255. (c) Sinha, A. K.; Seelan, S.; Tsubota, S.; Haruta, M. *Angew. Chem., Int. Ed.* **2004**, *43*, 1546–1548. (d) Hughes, M. D.; Xu, Y.-J.; Jenkins, P.; McMorn, P.; Landon, P.; Enache, D. I.; Carley, A. F.; Attard, G. A.; Hutchings, G. J.; King, F.; Stitt, H.; Johnston, P.; Griffin, K.; Kiely, C. J. *Nature* **2005**, *437*, 1132–1135.

(18) (a) Foss, C. A., Jr.; Hornyak, G. L.; Stoeckert, J. A.; Martin, C. R. *J. Phys. Chem.* **1994**, *98*, 2963–2971. (b) Martin, C. R. *Science* **1994**, *266*, 1961–1966. (c) Martin, C. R. *Chem. Mater.* **1996**, *8*, 1739–1746. (d) Nicewarner-Pena, S. R.; Freeman, R. G.; Reiss, B. D.; He, L.; Pena, D. J.; Walton, I. D.; Cromer, R.; Keating, C. D.; Natan, M. J. *Science* **2001**, *294*, 137–141.

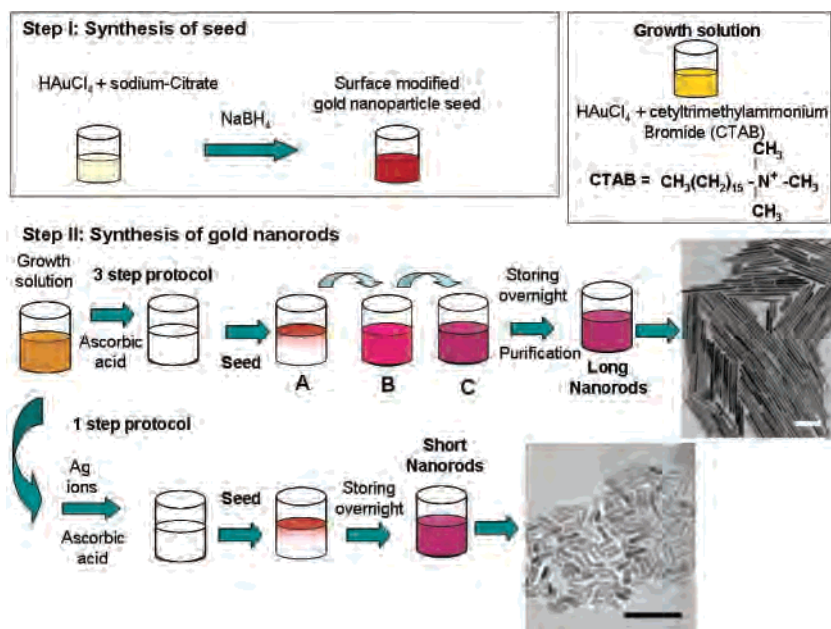


Figure 2. Schematic of the seed-mediated growth of gold nanorods developed in our laboratory.²² The seed is modified with citrate in this example, but other salts or molecules (e.g., thiols, surfactants) have been used at this point. Subsequently, a growth solution of more metal salt and surfactant, CTAB, is prepared, to which is added a weak reducing agent (ascorbic acid), followed by the seed. Upon addition of ascorbic acid, the growth solution turns from orange to colorless, indicating a reduction of gold(III) to gold(I). In the three-step seeding protocol that yields long gold nanorods, A–C are each growth solutions; the seed is added to A, and then after the color changes, an aliquot of solution A is added to B, etc. For short gold nanorods, silver nitrate and ascorbic acid are added to the growth solution, followed by the seed solution. Shown at the right are TEM micrographs of the final purified (centrifuged and washed) gold nanorod products. Scale bars represent 200 nm. See ref 22 for synthetic details.

1 (sphere) and ~ 25 . Even here, the literature is full of examples. One of the earliest approaches, demonstrated by Wang et al., employs electrochemical methods to generate gold nanorods in the presence of surfactants.²⁰ In this method, a gold plate is immersed in an aqueous electrolyte solution containing a mixture of surfactants such as cetyltrimethylammonium bromide (CTAB) and tetraoctylammonium bromide (TOAB).²⁰ Gold is oxidized to ions at the anode that are rereduced back to gold metal at the cathode but now in the form of nanorods. The length of the gold nanorods can be controlled by changing the ratio between the surfactant and the cosurfactant. Esumi, Yang, and others have demonstrated photochemical routes to gold nanorods.²¹ In these methods, gold salt is reduced in the presence of surfactants by UV irradiation, although it is not clear what is being oxidized in response.²¹

In our laboratory, we have developed a seed-mediated synthesis of gold nanorods in the presence of surfactants.²² This synthesis is performed in water, in air, and at room temperature and thus is amenable, in principle, to scaling up without the use of specialized equipment or organic solvents. Typically, a metal salt of gold (HAuCl_4) or silver (AgNO_3) is initially reduced by a strong reducing agent such as sodium borohydride to form spherical nanoparticles (more

properly, truncated single crystals that appear spherical by electron microscopy) in water. These spherical nanoparticles can be used as seeds on which to grow nanorods. In the presence of more metal salt, surfactants, and additional but milder reducing agents such as ascorbic acid, metal reduced on the seeds grows into nanorods or nanowires (Figure 2). Here, the presence of the directing surfactant is critical to achieving nonspherical shapes. In this Forum Article, we call materials with aspect ratios between 1 and 5 “short nanorods”, materials with aspect ratios between 5 and 25 “long nanorods”, and higher-yet-aspect-ratio materials “nanowires”, although this is by no means uniform in the literature.

In our method, a variety of synthetic parameters can be changed, leading to a change in the shape, yield, and size of the gold nanorods prepared. For example, the seed to the metal salt ratio limits how long the nanorod can grow.²² For gold, an aspect ratio of ~ 25 is the largest routinely observed by us. The size and nature of the seed could, in principle, be varied to give a range of gold nanorod aspect ratios; indeed, modest effects have been observed.²²¹ The nature of

- (19) (a) Walter, E. C.; Murray, B. J.; Favier, F.; Kaltenpoth, G.; Grunze, M.; Penner, R. M. *J. Phys. Chem. B* **2002**, *106*, 11407–11411. (b) Gates, B. D.; Xu, Q. B.; Stewart, M.; Ryan, D.; Willson, C. G.; Whitesides, G. M. *Chem. Rev.* **2005**, *105*, 1171–1196.
 (20) (a) Ying, Y.; Chang, S. S.; Lee, C. L.; Wang, C. R. C. *J. Phys. Chem. B* **1997**, *101*, 6661–6664. (b) Wang, Z. L.; Mohamed, M. B.; Link, S.; El-Sayed, M. A. *Surf. Sci.* **1999**, *440*, L809–L814.
 (21) (a) Esumi, K.; Matsuhisa, K.; Torigoe, K. *Langmuir* **1995**, *11*, 3285–3287. (b) Kim, F.; Song, J. H.; Yang, P. *J. Am. Chem. Soc.* **2002**, *124*, 14316–14317.

- (22) (a) Jana, N. R.; Gearheart, L.; Murphy, C. J. *Adv. Mater.* **2001**, *13*, 1389–1393. (b) Jana, N. R.; Gearheart, L.; Murphy, C. J. *J. Phys. Chem. B* **2001**, *105*, 4065–4067. (c) Jana, N. R.; Gearheart, L.; Murphy, C. J. *Chem. Commun.* **2001**, 617–618. (d) Murphy, C. J.; Jana, N. R. *Adv. Mater.* **2002**, *14*, 80–82. (e) Johnson, C. J.; Dujardin, E.; Davis, S. A.; Murphy, C. J.; Mann, S. *J. Mater. Chem.* **2002**, *12*, 1765–1770. (f) Busbee, B. D.; Obare, S. O.; Murphy, C. J. *Adv. Mater.* **2003**, *15*, 414–416. (g) Caswell, K. K.; Bender, C. M.; Murphy, C. J. *Nano Lett.* **2003**, *3*, 667–669. (h) Gao, J.; Bender, C. M.; Murphy, C. J. *Langmuir* **2003**, *19*, 9065–9070. (i) Sau, T. K.; Murphy, C. J. *Mater. Res. Soc. Symp. Proc.* **2004**, *789*, 203–212. (j) Sau, T. K.; Murphy, C. J. *Langmuir* **2004**, *20*, 6416–6420. (k) Sau, T. K.; Murphy, C. J. *J. Am. Chem. Soc.* **2004**, *126*, 8648–8649. (l) Gole, A.; Murphy, C. J. *J. Mater. Chem.* **2004**, *16*, 3633–3640. (m) Murphy, C. J.; Sau, T. K.; Gole, A.; Orendorff, C. J. *MRS Bull.* **2005**, *30*, 349–355. (n) Gou, L.; Murphy, C. J. *Chem. Mater.* **2005**, *17*, 3668–3672.

the directing surfactant used to control the shape can certainly be varied and greatly influences the final shape of the metal nanoparticles.^{15c,22h} In particular, in our laboratory, we are coming to the conclusion that bromide may be the most important part of the directing surfactant CTAB, despite our initial thoughts that rodlike micelles of CTA⁺ would serve as a soft template for the growth of metal nanorods.^{15c,22} The oxidation product(s) of the reaction—the oxidation products of ascorbic acid in our case—are also present in the reaction mixture as the nanoparticles grow, and their interaction with the gold surface is unclear, but their presence can also influence the course of the reaction.²²ⁿ On top of all of these mutually interdependent parameters, additives such as other metal salts influence the crystal growth and morphology of the nanoparticles. For example, addition of silver ions to the reaction mixture to make gold nanorods significantly increases the yield of the gold nanorods but limits the achievable aspect ratios to ~ 6 (Figure 2).^{22j,23} The general concept that the crystal shape and habit can be controlled through manipulation of relative surface energies is familiar, but its practical demonstration, via preferential adsorption of additives under certain reaction conditions, is gaining momentum in the nanomaterials literature.²⁴

To rationally control the nanocrystal shape, an understanding of the growth mechanism is essential. A number of techniques, such as electron diffraction (ED) of single nanorods and high-resolution electron microscopy, can provide information on the nature of the crystal faces along each axis of the final, or perhaps intermediate, material. Thermal analysis and surface charge measurements of the final products can provide information about the nature and amount of adsorbed organics, or ions, on the nanocrystal surface; if one is fortunate to have enough sample, NMR spectra of adsorbed organics can be obtained. Spectroscopic analyses as a function of time, should intermediates have distinct absorption bands, provide kinetic data. Many workers, in fact, are doing these types of experiments now and are pushing the limits of achievable aspect ratios and purity of gold nanorods/nanowires.^{15,22–28} On the basis of our own experience, a number of parameters are individually and

simultaneously responsible for the final shape and size of the gold nanorods. For instance, in Figure 2, we currently believe that, after the gold seed has been added to the growth solution (without silver ion present), bromide chemisorbs with some small preference to the future side faces of gold, which in turn recruits the cationic surfactant, with some small preference, to those faces; if the surfactant tails are sufficiently long, a bilayer is formed at those faces, blocking growth there and leading to anisotropic crystal growth. However, because the preference for bromide for one face over another is not large, other nanoparticle shapes do appear in the pot and need to be purified away by washing and centrifugation steps. Hence, the final state of the nanocrystals depends on a number of factors working synergistically and dynamically in time: the nature of the counterion, the size of the surfactant headgroup, and the length of the surfactant tail, not to mention the relative concentrations of all species, pH, temperature, and strength of the reducing agent in the growth step.^{15c}

El-Sayed and co-workers have used thermogravimetric analysis to quantitate the amount of surfactant on the surface of gold nanorods.²³ Coupled with Fourier transform infrared measurements, they established that the surfactant is associated with gold nanorods in the form of a bilayer. The CTAB binding is thought to place via a gold–bromide surfactant complex. The bromide ion is thought to be the bridge between the gold surface and the positively charged quaternary nitrogen of the surfactant.²³ Theoretical and vibrational studies for CTAB on silver nanoparticles suggest that bromide is indeed chemisorbed, although those data also suggest that CTAB's surfactant tail lies parallel to the silver surface, not perpendicular.²⁷ The ζ potential (effective surface charge) of long gold nanorods, in water, as determined by us was found to be $\sim +30$ mV, consistent with the cationic portion of the surfactant dominating the nanorods but not exactly consistent with a strongly bound layer of bromide. Nonetheless, if the bromide counterion of CTAB is replaced with chloride, no gold nanorods are found,^{15c,22} hence our emphasis in the mechanism for the role of the counterion as the first step.

Recently, Perez-Juste et al. have proposed an electric-field-directed mechanism for the growth of gold nanorods.²⁵ In this mechanism, gold(I) ions are bound to the CTAB micelles and are transported to the growing seed particles. This transport is controlled by the double-layer interaction and hence is field-directed. The field at the tips of the rods is larger, compared to the sides, and this leads to the preferential attachment of ions on the tips, leading to the elongation of the particles. Indeed, experiments to distinguish between this scenario and preferential adsorption of ions are difficult to evaluate in the highly concentrated surfactant environment

- (23) (a) Nikoobakht, B.; El-Sayed, M. A. *Chem. Mater.* **2003**, *15*, 1957–1962. (b) Nikoobakht, B.; El-Sayed, M. A. *Langmuir* **2001**, *17*, 6368–6374. (c) Nikoobakht, B.; Wang, J.; El-Sayed, M. A. *Chem. Phys. Lett.* **2002**, *366*, 17–23.
- (24) (a) Siegfried, M. J.; Choi, K.-S. *Adv. Mater.* **2004**, *16*, 1743–1746. (b) Siegfried, M. J.; Choi, K.-S. *Angew. Chem., Int. Ed.* **2005**, *44*, 3218–3223. (c) Song, H.; Kim, F.; Connor, S.; Somorjai, G. A.; Yang, P. D. *J. Phys. Chem. B* **2005**, *109*, 188–193. (d) Wiley, B.; Sun, Y.; Xia, Y. *Langmuir* **2005**, *21*, 8077–8080. (e) Wiley, B.; Herricks, T.; Sun, Y.; Xia, Y. *Nano Lett.* **2004**, *4*, 1733–1739. (f) Herricks, T.; Chen, J.; Xia, Y. *Nano Lett.* **2004**, *4*, 2367–2371. (g) Pillai, Z. S.; Kamat, P. V. *J. Phys. Chem. B* **2004**, *108*, 945–951. (h) Colfen, H. *Curr. Opin. Colloid Interface Sci.* **2003**, *8*, 23–31. (i) Filankembo, A.; Giorgio, S.; Lisiecki, I.; Pileni, M. P. *J. Phys. Chem. B* **2003**, *107*, 7492–7500. (j) Leontidis, E.; Kleitou, K.; Kyprianidou-Leodidou, T.; Belkiari, V.; Lianos, P. *Langmuir* **2002**, *18*, 3659–3668.
- (25) (a) Perez-Juste, J.; Liz-Marzan, L. M.; Carnie, S.; Chan, D. Y. C.; Mulvaney, P. *Adv. Funct. Mater.* **2004**, *14*, 571–579. (b) Rodriguez-Fernandez, J.; Perez-Juste, J.; Mulvaney, P.; Liz-Marzan, L. M. *J. Phys. Chem. B* **2005**, *109*, 14257–14261.
- (26) Liu, M.; Guyot-Sionnest, P. *J. Phys. Chem. B* **2005**, *109*, 22192–22200.
- (27) Koglin, E.; Tarazona, A.; Kreising, S.; Schwuger, M. J. *Colloids Surf. A* **1997**, *123*, 523–542.

- (28) (a) Lofton, C.; Sigmund, W. *Adv. Funct. Mater.* **2005**, *15*, 1197–1208. (b) Hernandez, J.; Solla-Gullon, J.; Herrero, E.; Aldaz, A.; Feliu, J. M. *J. Phys. Chem. B* **2005**, *109*, 12651–12654. (c) Wei, Z. Q.; Zamborini, F. P. *Langmuir* **2004**, *20*, 11301–11304. (d) Liao, H. W.; Hafner, J. H. *J. Phys. Chem. B* **2004**, *108*, 19276–19280. (e) Niidome, Y.; Nishioka, K.; Kawasaki, H.; Yamada, S. *Chem. Commun.* **2003**, 2376–2377. (f) Jana, N. R. *Small* **2005**, *1*, 875–882. (g) Chen, H. M.; Peng, H.-C.; Liu, R.-S.; Asakura, K.; Lee, C.-L.; Lee, J.-F.; Hu, S.-F. *J. Phys. Chem. B* **2005**, *109*, 19553–19555.

in which these syntheses are conducted. More recently, the contribution of silver ions to the control of gold nanorod structures has been examined by Liu and Guyot-Sionnest, who suggest that silver(I) is deposited and reduced preferentially at certain crystal faces of the gold particle, slowing down growth on those faces and leading to anisotropic shapes.²⁶

Are gold nanorods single crystalline, polycrystalline, or "other"? We have performed high-resolution transmission electron microscopy (TEM) studies along with selective-area ED to determine the nature of the faces of long gold nanorods prepared by the three-step seeding protocol, without silver ion present.^{22e} The ED patterns showed penta-tetrahedral twinned particles. The side faces were found to be (somewhat ambiguously) {100} or {110} or a combination of both; more clearly, the nanorod ends consisted of five tetrahedra making a ring, to expose five triangular {111} faces at the end of each of the rods.^{22e} The seed particles appeared to be single crystals; therefore, our proposal is that, at an early stage, the face-centered-cubic symmetry of gold is broken by twinning to produce multiply twinned particles that are formed from these seeds as metal salt is reduced. At this stage, preferential binding of the surfactant CTAB on the {100} or {110} side faces leads to the blocking of the long faces and the rods elongate. Gai and Harmer²⁹ have studied long gold nanorods formed by our seed-mediated method. Their atomic resolution findings indicate the presence of multiply twinned particles dominated by decahedral and icosahedral shapes and lead to a similar conclusion: the long gold nanorods are twinned defect structures in which the side faces are {110} and {111} at the ends. Analogous data to support 5-fold twinning in silver nanorods and nanowires have been reported by others.³⁰ How this general structure of gold nanorods may be different, depending on the presence of additive ions, is still emerging.^{15,22,26} It is clear that ideas about a *general* mechanism of nanorod formation, even for gold, have not converged, or if ideas have converged, the words used to describe these ideas have not converged. For example, some would say that the notion of preferential binding of additives to certain crystal faces is thermodynamic control of crystal growth, whereas others would just as readily call this kinetic control of crystal growth.^{2,22–28} More rigorous characterization studies as a function of time are needed to support or refute proposed mechanisms; recent developments in electron microscopy in which elemental analyses can be done at the near-atomic scale are likely to be very helpful. Relatively scarce is work on computer simulations of crystal growth for these materials, with parameters that would help to distinguish between various complex possibilities.

II.B. Silver. Like gold, silver nanoparticles have brilliant colors in the visible and near-infrared region of the EM spectrum that vary with shape and size. Its high electrical

conductivity in the bulk, coupled with its cheaper raw materials, has led many workers to examine silver instead of gold, despite its lesser chemical stability in air compared to gold.^{10,22,30,31}

Strategies to control the growth of anisotropic silver nanoparticles have involved templating against various types of 1-D structures, such as channels in alumina or other membranes,^{32a} mesoporous materials,^{32b} carbon nanotubes,^{32c} block copolymers,^{32d} DNA chains,^{32e,f} and peptide fibrils.^{32g} Good control over nanoparticle dimensions can be achieved through these routes, but some purification steps are required to retrieve the silver nanowires. Xia and co-workers have demonstrated a hot-solution approach based on the polyol process for the large-scale synthesis of silver nanowires, 30–60 nm in diameter, which is somewhat tunable, and 1–50 μm in length.^{10,33} Silver nanowires are produced when AgNO_3 is reduced in the presence of the capping/directing agent poly(vinylpyrrolidone) by ethylene glycol, which is both the solvent and reductant, in the presence of either platinum or silver seeds.³³ The preparation does yield other shapes of silver nanoparticles, as described above for gold nanorods, but smaller colloidal particles can be removed by centrifugation and washing steps. Many researchers are still finding solution conditions to prepare silver nanowires; a recent example is a colloidal route to silver nanowires with high aspect ratios (8–10 nm in diameter and lengths up to 10 μm) that involves the reduction of AgNO_3 with Vitamin C in sodium dodecyl sulfate/ethanol solutions.³⁴ The crystalline nature of silver nanowires prepared by these various groups has been examined in some cases, and reports of both single-crystalline wires and twinned wires can be found.^{10,30,33,34}

The synthesis of 1-D silver nanorods of controllable aspect ratio has been reported by our group, using analogous silver salts per Figure 2.^{22c} In that method, the presence of seeds and surfactants is very important in controlling crystal growth, but it was also possible, through slight changes in the reaction conditions, to produce wires with an uncontrolled aspect ratio (~ 50 – 350). More recently, however, we found that silver nanowires can be made in very high yield, albeit with no good control over the aspect ratio (diameters 25–32 nm; lengths up to 18 μm) by boiling aqueous silver nitrate solutions with sodium citrate and sodium hydroxide aqueous

(29) Gai, P. L.; Harmer, M. A. *Nano Lett.* **2002**, *2*, 771–774.

(30) (a) Sun, Y.; Mayers, B.; Herricks, T.; Xia, Y. *Nano Lett.* **2003**, *3*, 955–960. (b) Ni, C. Y.; Hassan, P. A.; Kaler, E. W. *Langmuir* **2005**, *21*, 3334–3337. (c) Zhang, S. H.; Jiang, Z. Y.; Xie, Z. X.; Xu, X.; Huang, R. B.; Zheng, L. S. *J. Phys. Chem. B* **2005**, *109*, 9416–9421. (d) Sun, X.; Li, Y. *Adv. Mater.* **2005**, *17*, 2626–2630.

(31) (a) Dickson, R. M.; Lyon, L. A. *J. Phys. Chem. B* **2000**, *104*, 6095–6098. (b) Jin, R. C.; Cao, Y. W.; Mirkin, C. A.; Kelly, K. L.; Schatz, G. C.; Zheng, J. G. *Science* **2001**, *294*, 1901–1903. (c) Mock, J. J.; Oldenburg, S. J.; Smith, D. R.; Schultz, D. A.; Schultz, S. *Nano Lett.* **2002**, *2*, 465–469. (d) Sun, Y.; Xia, Y. *Adv. Mater.* **2002**, *14*, 833–837.

(32) (a) Zhang, Z.; Gekhtman, D.; Dresselhaus, M. S.; Ying, J. Y. *Chem. Mater.* **1999**, *11*, 1659–1665. (b) Han, Y. J.; Kim, J. M.; Stucky, G. D. *Chem. Mater.* **2000**, *12*, 2068–2069. (c) Ugarte, D.; Chatelein, A.; de Heer, W. A. *Science* **1996**, *274*, 1897–1899. (d) Zhang, D.; Qi, L.; Ma, J.; Cheng, H. *Chem. Mater.* **2001**, *13*, 2753–2755. (e) Braun, E.; Eichen, Y.; Sivan, U.; Ben-Joseph, G. *Nature* **1998**, *391*, 775–778. (f) Yan, H.; Park, S. H.; Finkelstein, G.; Reif, J. H.; LaBean, T. H. *Science* **2003**, *301*, 1882–1884. (g) Reches, M.; Gazit, E. *Science* **2003**, *300*, 625–627.

(33) (a) Sun, Y.; Gates, B.; Mayers, B.; Xia, Y. *Nano Lett.* **2002**, *2*, 165–168. (b) Sun, Y.; Xia, Y. *Adv. Mater.* **2002**, *14*, 833–837. (c) Sun, Y.; Yin, Y.; Mayers, B. T.; Herricks, T.; Xia, Y. *Chem. Mater.* **2002**, *14*, 4736–4745.

(34) Liu, Y.; Chu, Y.; Yang, L.; Han, D.; Lü, Z. *Mater. Res. Bull.* **2005**, *40*, 1796–1801.

solutions.³⁵ Because the concentration of sodium hydroxide is critical to producing silver nanowires, we currently think of adsorbed hydroxide as the key factor in controlling crystal growth under these conditions.³⁵ This notion highlights, again, the concept of adsorbed ions blocking reactions on one face of a growing nanocrystal to control the crystal shape; in this case, no surfactant, seeds, micelles, etc., are present at all. The ease of preparation of silver nanowires under these conditions makes scaling up of the process more feasible.

III. Surface Functionalization of Metallic Nanorods/Nanowires

Given that one can prepare gold and silver nanorods or nanowires with control over their dimensions, chemists can readily imagine wanting to functionalize their surfaces for various applications. A key question, then, is, what is on the particle surface initially, after synthesis and purification? Another key question is, how can the surface be modified? This second question is, in general, easier to answer: thiols, and disulfides, on gold surfaces are well-known to form self-assembled monolayers because of the relative strength of the Au–S bond.³⁶ Similarly, thiols, and amines, are known to bind well to silver surfaces. Therefore, gold and silver nanoparticles are frequently exposed to thiols, disulfides, or amines, with reasonable expectations of surface modification by them. However, given that there is almost always something—surfactant, polymer, adsorbed ions at the very least—on metallic nanoparticles made by the types of colloidal routes described above, one has to consider displacement of these species before thiols or amines might bind.

What kinds of applications are possible by controlling the surface chemistry of a nanoparticle? One example is a solution-based colorimetric sensor, in which the controlled aggregation of surface-modified gold nanospheres by the addition of analyte results in a color change from orange-pink to blue-gray.³⁷ Fundamentally, this effect is due to plasmon coupling between nearby particles, and the distance dependence of this phenomenon is being explored as a spectroscopic ruler for assorted applications.³⁸ If biomolecules such as proteins or DNA are used for the surface modification or for the bridging analyte, then nanoparticle-based bioassays are readily achievable.³⁷ The chemical modification of colloidal metal nanospheres has been well studied.³⁹ It is only recently that attempts have been made

Table 1. Examples of Surface Functionalization of Gold Nanorods

coating material	coating thickness	ref
mercaptopropionic acid	typical monolayer dimensions (~1 nm)	40a
MPTMS	typical monolayer dimensions (~1 nm)	40c
DNA	6 nm	40e
polyelectrolyte (lbl assembly)	~2 nm per single polymer layer	40j
silica	variable thickness	40b–d
silver	variable thickness	40m–o

to modify the surface of 1D colloidal metal nanorods and nanowires. Both organic (soft) and inorganic (hard) materials have been utilized as coatings; Table 1 gives some examples.⁴⁰ Small organic molecules such as mercaptopropionic acid have been preferentially attached to gold nanorod ends, presumably because of the thiol affinity for gold; the preference for end-face binding likely comes about as a result of blocking of the side faces by the surfactants used in the synthesis.^{40a} We have also demonstrated the surface modification of gold nanorods by biotin disulfide, a slightly larger organic molecule, either preferentially onto the nanorod ends^{40k} (again, most likely as a result of blocking of the side faces by the directing surfactant) or onto the entire gold nanorod surface.^{40l} In this latter example, we overcoated with cationic CTAB bilayer and with anionic poly(acrylic acid) in an electrostatic layer-by-layer approach and reacted the acid groups with a biotin-amine to functionalize the whole surface. The layer-by-layer electrostatic assembly of polymers approach has numerous antecedents in a number of laboratories: Caruso and co-workers have demonstrated it for spherical nanoparticles and also for nickel nanorods.^{40h,i} We have extended this technique to uniformly coat polymer multilayers onto the gold nanorod surface.^{40j} Biological molecules are increasingly popular choices for coating gold nanorods. In fact, we have done this indirectly by using the well-known affinity of the protein streptavidin to bind up to four biotins very tightly and linked gold nanorods via biotin–streptavidin connectors.^{40k,l} Mann, Mallouk, and others have attached DNA to nanorods/nanowires surfaces.^{40e,f} Chang et

- (35) Caswell, K. K.; Bender, C. M.; Murphy, C. J. *Nano Lett.* **2003**, *3*, 667–669.
 (36) Checkic, V.; Crooks, R. M.; Stirling, C. J. M. *Adv. Mater.* **2000**, *12*, 1161–1171.
 (37) (a) Elghanian, R.; Storhoff, J. J.; Mucic, R. C.; Letsinger, R. L.; Mirkin, C. A. *Science* **1997**, *277*, 1078–1081. (b) Taton, T. A.; Mirkin, C. A.; Letsinger, R. L. *Science* **2000**, *289*, 1757–1760. (c) Kim, Y.; Johnson, R. C.; Hupp, J. T. *Nano Lett.* **2001**, *1*, 165–167. (d) Thanh, N. T. K.; Rosenzweig, Z. *Anal. Chem.* **2002**, *74*, 1624–1628. (e) Obare, S. O.; Hollowell, R. E.; Murphy, C. J. *Langmuir* **2002**, *18*, 10407–10410.
 (38) (a) Su, K. H.; Wei, Q. H.; Zhang, X.; Mock, J. J.; Smith, D. R.; Schultz, S. *Nano Lett.* **2003**, *3*, 1087–1090. (b) Sonnichsen, C.; Reinhard, B. M.; Liphardt, J.; Alivisatos, A. P. *Nat. Biotechnol.* **2005**, *23*, 741–745. (c) Reinhard, B. M.; Siu, M.; Agarwal, H.; Alivisatos, A. P.; Liphardt, J. *Nano Lett.* **2005**, *5*, 2246–2252.

- (39) (a) Templeton, A. C.; Wuelfing, W. P.; Murray, R. W. *Acc. Chem. Res.* **2000**, *33*, 27–36. (b) Shanhar, R.; Rotello, V. M. *Acc. Chem. Res.* **2003**, *36*, 549–561. (c) Verma, A.; Rotello, V. M. *Chem. Commun.* **2005**, 303–312.
 (40) (a) Thomas, K. G.; Barazzouk, S.; Ipe, B. I.; Joseph, S. T. S.; Kamat, P. V. *J. Phys. Chem. B* **2004**, *108*, 13066–13068. (b) Chang, S. S.; Shih, C. W.; Chen, C. D.; Lai, W. C.; Wang, C. R. C. *Langmuir* **1999**, *15*, 701–709. (c) Obare, S. O.; Jana, N. R.; Murphy, C. J. *Nano Lett.* **2001**, *1*, 601–603. (d) Boev, V. I.; Perez-Juste, J.; Pastoriza-Santos, I.; Silva, C. J. R.; de Gomes, M.; Liz-Marzan, L. M. *Langmuir* **2004**, *20*, 10268–10272. (e) Dujardin, E.; Hsin, L.-B.; Wang, C. R. C.; Mann, S. *Chem. Commun.* **2001**, 1264–1265. (f) Mbindyo, J. K. N.; Reiss, B. D.; Martin, B. R.; Keating, C. D.; Natan, M. J.; Mallouk, T. E. *Adv. Mater.* **2001**, *13*, 249–254. (g) Chang, J.-Y.; Wu, H.; Chen, H.; Ling, Y.-C.; Tan, W. *Chem. Commun.* **2005**, 1092–1094. (h) Gittins, D. I.; Caruso, F. *J. Phys. Chem. B* **2001**, *105*, 6846–6852. (i) Mayya, K. S.; Gittins, D. I.; Dibaj, A. M. *Nano Lett.* **2001**, *1*, 727–730. (j) Gole, A.; Murphy, C. J. *Chem. Mater.* **2005**, *17*, 1325–1330. (k) Caswell, K. K.; Wilson, J. N.; Bunz, U. H. F.; Murphy, C. J. *J. Am. Chem. Soc.* **2003**, *125*, 13914–13915. (l) Gole, A.; Murphy, C. J. *Langmuir* **2005**, *21*, 10756–10762. (m) Ah, C. S.; Hong, S. D.; Jang, D. J. *J. Phys. Chem. B* **2001**, *105*, 7871–7873. (n) Liu, M.; Guyot-Sionnest, P. *J. Phys. Chem. B* **2004**, *108*, 5882–5888. (o) Huang, C. C.; Yang, Z.; Chang, H. T. *Langmuir* **2004**, *20*, 6089–6092.

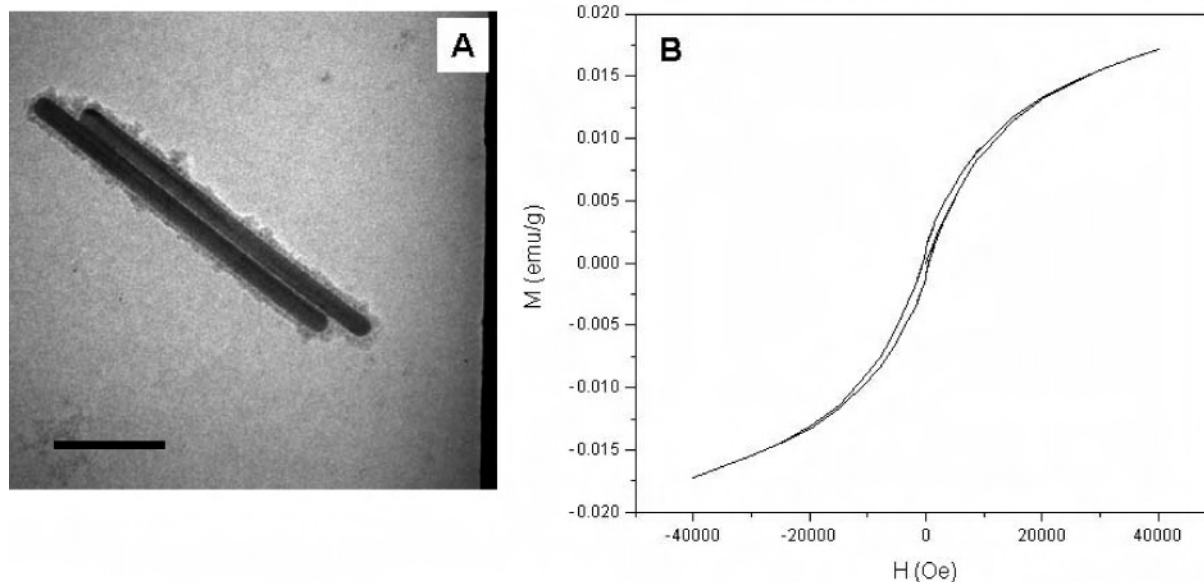


Figure 3. (A) TEM micrograph of gold nanorods coated with a layer of iron oxide. Scale bar = 100 nm. (B) Magnetization versus magnetic field (hysteresis curve) for iron oxide nanoparticle coated gold nanorods at $T = 2$ K.

al. have bound antimouse IgG specifically to the gold nanorod ends. They further use the protein mouse IgG to achieve oriented assembly of nanorods in solution.^{40g}

Numerous groups have shown gold nanorod functionalization by silanes and subsequent formation of silica coatings.^{40b–d} This is a simple process wherein the particles are first modified by a monolayer of silane. Typically, these silanes have thiols at one end that bind to gold, and the terminal functionality is a precursor that is further reacted to grow a silica shell. An example of a good silane for this purpose is (3-mercaptopropyl)trimethoxysilane (MPTMS), $\text{HSCH}_2\text{CH}_2\text{CH}_2\text{Si}(\text{OCH}_3)_3$. The addition of sodium silicate under appropriate conditions and storing for certain period of time give rise to a shell of silica around the particles. This shell dimension can be controlled by variation of certain parameters. Reduction of silver salt on the surface of the gold nanorods has been done to achieve Ag@Au shell–core nanorods. The reduction is carried out by different reducing agents such as hydroxylamine or ascorbic acid. The thickness can also be controlled by appropriate choices of reactants.^{40m–o}

We present here some new data on hard shell coatings of gold nanorods to illustrate the interesting possibilities one has with surface chemistry. The goal of these experiments was to make magnetically addressable gold nanorods; the approach was to coat gold nanorods with magnetite, Fe_3O_4 . We were unable to obtain reproducible results by adding premade Fe_3O_4 nanoparticles (diameter ~ 10 nm) to gold nanorods and, therefore, turned to an in-situ growth method. Long gold nanorods were synthesized by our three-step protocol (Figure 1)²² and further coated with a single layer of the polymer poly(styrene sulfonate), which is anionic and thus is electrostatically associated with the cationic CTAB-coated gold nanorods.^{40j} This solution was then reacted with a solution containing iron(II) and iron(III) ions (molar ratio: 0.5), followed by NaOH to produce Fe_3O_4 , similar to established protocols for “ferrofluid”.⁴¹ The solutions of the final product could easily be moved with external magnetic

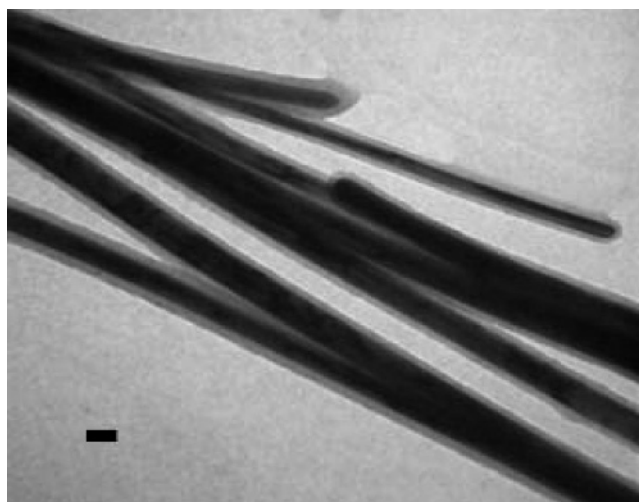


Figure 4. TEM micrograph of silica on silver nanowires. Scale bar: 40 nm.

fields (e.g., a magnetic stir bar), suggesting that magnetite was present. TEM micrographs (Figure 3A) show the somewhat homogeneous outer coating around the gold nanorod templates that is presumably magnetite. Magnetic measurements indicated that the composite showed magnetic properties consistent with those of magnetite (Figure 3B). A further detailed investigation is being carried out in the laboratory at the present time.

Analogous experiments to functionalize silver nanowires with a layer of SiO_2 have been achieved in our laboratory. Our approach starts with the standard bifunctional precursor, MPTMS, which binds to the silver surface via the thiol group. A thin SiO_2 layer is subsequently grown on the MPTMS layer through a modified Stöber method using sodium silicate (Figure 4).^{40c} The thickness of the layer can be controlled from approximately 9 to 150 nm by adjusting the growth conditions. Dissolution of the inner silver core with aqueous

(41) Breitzer, J.; Lisensky, G. C. *J. Chem. Educ.* **1999**, *76*, 943–948.

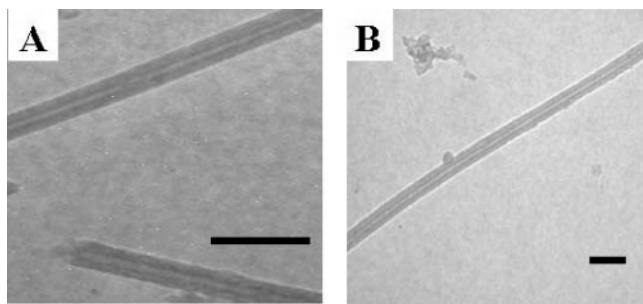
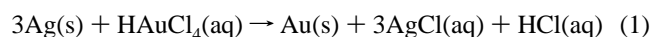


Figure 5. TEM micrographs of hollow silica nanotubes after dissolution of the inner silver core, with aqueous ammonia. Scale bars: 100 nm.

ammonia can yield hollow silica nanotubes of very high aspect ratio; we had already demonstrated the analogous dissolution reaction of gold nanorods encased in a silica shell, using cyanide.^{40c} As shown in Figure 5, the silica nanotubes obtained using this procedure are smooth and uniform and the inner diameter is controlled by the diameter of the original silver nanowire template.

In more work that we present here for the first time, we have been able to make gold sheaths around silver nanowires. The experiments are analogous to that of Sun and Xia, who made silver nanocubes and then grew gold nanoboxes around them.⁴² In our case, this is the only way we have been able to make gold nanowires (albeit hollow ones), with bimetallic gold–silver nanowires as intermediates. We began with silver nanowires prepared through a seedless, surfactantless method.^{22g} The addition of HAuCl_4 to the silver nanowire solution results in a galvanic replacement reaction according to⁴²



TEM was used to follow the morphological changes at various stages of the replacement reaction between silver nanowires and HAuCl_4 . Initially, when less than stoichiometric amounts of HAuCl_4 were added, we noticed that pits formed on the silver; we speculate that these newly formed surfaces would be the most active sites for further reaction. With sufficient gold salt, the silver is reacted and bimetallic hollow nanotubes are left behind; ultimately, in principle, pure gold nanotubes are achievable. Figure 6 shows TEM micrographs of partially reacted silver nanowires with gold salt; the materials are hollow, and both gold and silver are present according to energy-dispersive X-ray microanalysis (EDAX) after washing. We also monitored the galvanic replacement reaction between silver nanowires and the HAuCl_4 solution by UV–vis absorption spectroscopy, and the results showed a strong dependence of the spectra on their shape and structure. During the course of the reaction, we observed a significant decrease for the silver transverse plasmon peak at 370 nm, while the gold plasmon band at longer wavelength (>520 nm) displayed a significant increase. The peak at 520 nm for gold continued to increase in intensity and red-shift to ~ 550 nm as more aqueous HAuCl_4 solution was added to the reaction system. This red

(42) Sun, Y.; Xia, Y. *Science* **2002**, *298*, 2176–2179.

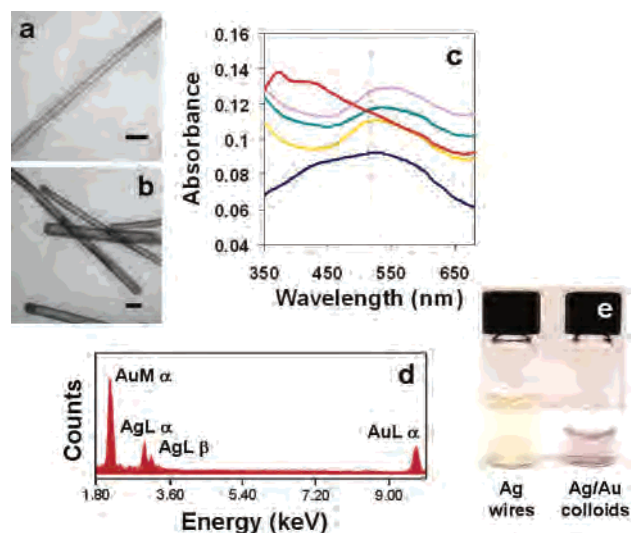


Figure 6. (a and b) TEM micrographs of silver/gold bimetallic colloids with ~ 19 -nm wall thickness. Scale bars = 100 nm. (c) Absorbance spectra of silver nanowires (red trace), silver/gold colloids with wall thickness ~ 13 nm (navy blue trace), ~ 19 nm (orange trace), ~ 27 nm (green trace), and ~ 31 nm (purple trace). (d) EDAX of silver/gold colloids. (e) Photograph of silver nanowires (left) and silver/gold colloids (right) with ~ 19 -nm wall thickness.

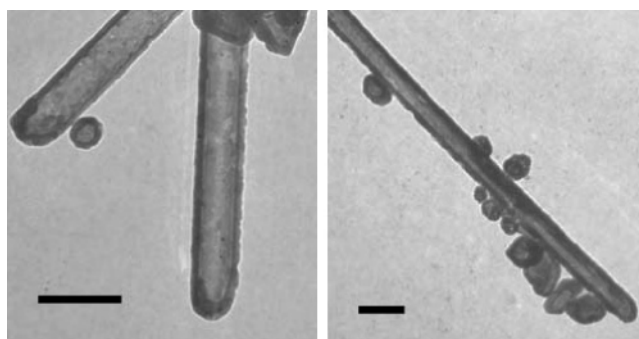


Figure 7. Hollow gold colloids after ammonia treatment. Scale bars = 200 nm.

shift in the gold plasmon peak position may reflect its morphology, as has been observed for gold nanoshells.⁴³

The as-prepared bimetallic colloids were then treated with ammonia, as with the silica-coated silver nanowires, to remove all of the silver and obtain high-aspect-ratio gold nanotubes (Figure 7). TEM micrographs show that the materials were indeed mostly hollow, and the wall thickness was decreased approximately 4 nm compared to the starting thickness of 19 nm.

IV. Novel Properties of Metallic Nanorods/Nanowires

IV.A. Optical Properties. Localized surface plasmon resonance (LSPR) of metal nanoparticles refers to the collective oscillation of electrons in the conduction band in resonance with incident radiation.^{4,5,44} For gold and silver, LSPR leads to strong plasmon absorption and Rayleigh scattering in the visible wavelength regime (Figure 1). Moreover, this electron oscillation is restricted by the size and shape of the metal nanoparticle, which gives rise to the

(43) Oldenburg, S. J.; Averitt, R. D.; Westcott, S. L.; Halas, N. J. *Chem. Phys. Lett.* **1998**, *288*, 243–247.

(44) Hao, E.; Schatz, G. C. *J. Chem. Phys.* **2004**, *120*, 357–366.

size- and shape-dependent optical properties of gold and silver nanoparticles. Spherical silver and gold nanoparticles have a single plasmon absorption band at ~ 400 and ~ 510 nm, respectively. 1-D nanorods/nanowires of silver and gold have two principle plasmon bands. The band at higher energy corresponds to absorption and scattering along the short axis of the nanorod/nanowire, while the lower energy band corresponds to absorption and scattering along the long axis of the nanorod/nanowire. In addition, large local EM field enhancements at the ends of anisotropic nanoparticles shown in theoretical studies⁴⁴ make nanorods/nanowires attractive candidates as substrates for surface-enhanced Raman scattering (SERS).

IV.B. Electronic Properties. Much of the interest in 1-D metal nanowires is centered around incorporating these materials into microdevices/nanodevices. Construction of one such device has been reported by Heath and co-workers.⁴⁵ In this work, the authors were able to deposit a high-density electrode array of platinum nanowires on silicon substrates using the superlattice nanowire pattern transfer technique. The resulting device had a nanowire density of 60 wires per 100 μm with regular spacing and was used as a high-frequency nanomechanical resonator.

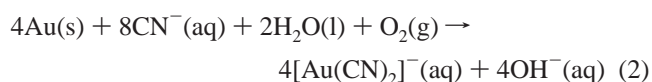
However, to understand the nanowire performance in these devices, it is important to understand the electrical properties of these materials. For example, Mallouk and co-workers⁴⁶ have developed a system for studying the fundamental electrical properties of gold nanowires by assembling them on interdigitated arrays of microscale electrodes to make electrical contacts. Using these assembled nanowire contacts, they determined the resistivity through individual nanowires. For 350-nm-diameter gold nanowires, the resistivity is $\sim 2.9 \times 10^{-6} \Omega \text{ cm}$, which is comparable to that of bulk gold.⁴⁶

There are examples of metal nanowires in chemical-sensing devices. While the resistance in semiconducting nanowires is quite responsive to chemisorbed ions from solution, charge screening near the metal nanowire surface renders them poor ion sensors. However, the resistance in metal nanowires is responsive to other chemical species. In separate reports, Tao et al.⁴⁷ have used gold nanowires (~ 1 nm in diameter and ~ 50 nm in length) and Penner et al.⁴⁸ have used silver nanowires as amine and ammonia sensors. In addition, Penner and co-workers⁴⁹ have used palladium nanowires grown at graphite step edges to detect hydrogen gas.

IV.C. Mechanical Properties. In addition to understanding the electrical properties of these materials for nanoscale devices, it is also important to study their mechanical and structural properties in order to properly evaluate the device

performance. Experimentally, the metal nanowire strength, elastic modulus, and hardness can be measured using a modified atomic force microscope or lateral force microscope. Boland et al.⁵⁰ measured the average yield strength of gold nanowires with diameters between 50 and 250 nm to be 5.6 GPa, which is 10 times greater than that of bulk gold (0.4 GPa). In addition, they found that gold nanowires do not exhibit the near-perfect elastoplasticity of nanoparticles but are more elastoplastic than bulk gold. The authors report comparable yield strengths for copper nanowires as well. Experiments from our group describe calculations of similar mechanical parameters for silver nanowires using nanoindentation techniques.⁵¹ In these experiments, we found the yield strength of silver nanowires with diameters of ~ 40 nm to be ~ 0.88 GPa, which is approximately twice that of bulk silver. These results indicate that nanowires are sufficiently robust to be applied toward working microdevices/nanodevices.

IV.D. Chemical Reactivity and Catalysis. Bulk noble metals, such as gold and silver, are relatively inert but can undergo complexation reactions, which cause dissolution. For example, gold can react with aqueous cyanide under ambient conditions to form a complex ion:⁵²



This reaction also takes place on the nanoscale for gold nanorods but is highly dependent on the nanorod aspect ratio.⁵³ Aspect ratio ~ 2 gold nanorods dissolve much faster (30 min) than aspect ratio ~ 20 rods (> 24 h) in aqueous cyanide. For short nanorods, the reaction occurs preferentially at the ends of the rods, rounding the rods down to spheres. The reaction of cyanide with longer gold nanorods occurs more readily along the long axis of the rod rather than the end, an observation that has yet to be satisfactorily explained—because thiols and disulfides apparently prefer to react at the ends of the nanorods rather than to go through the CTAB bilayer on the sides.^{40k} Although gold in the bulk is inert, recent reports provide evidence that it becomes catalytically active in the nanoscale regime.¹⁷

V. 1-D Metal Nanoparticle Arrays

V.A. End-to-End Organization of Nanorods. Fabricating 1-D arrays, or end-to-end assemblies, of nanorods is interesting for numerous sensing or electronic applications. In our group, we have prepared end-to-end assemblies of aspect ratio ~ 20 gold nanorods with biological linkers, biotin-streptavidin.^{40k} In these experiments, CTAB-protected nanorods were modified with a biotin disulfide. Upon the addition of streptavidin, a protein that is well-known to bind to up to four biotins, nanorods are linked end-to-end and

(45) Melosh, N. A.; Boukai, A.; Diana, F.; Gerardot, B.; Badolato, A.; Petroff, P. M.; Heath, J. R. *Science* **2003**, *300*, 112–115.

(46) Smith, P. A.; Nordquist, C. D.; Jackson, T. N.; Mayer, T. S.; Martin, B. R.; Mbindyo, J.; Mallouk, T. E. *Appl. Phys. Lett.* **2000**, *77*, 1399–1401.

(47) Li, C. Z.; He, H. X.; Bogozi, A.; Bunch, J. S.; Tao, N. J. *Appl. Phys. Lett.* **2000**, *76*, 1333–1335.

(48) Murray, B. J.; Newberg, J. T.; Walter, E. C.; Li, Q.; Hemminger, J. C.; Penner, R. M. *Anal. Chem.* **2005**, *77*, 5204–5214.

(49) Favier, F.; Walter, E. C.; Zach, M. P.; Benter, T.; Penner, R. M. *Science* **2001**, *293*, 2227–2231.

(50) Wu, B.; Heidelberg, A.; Boland, J. J. *Nat. Mater.* **2005**, *4*, 525–529.

(51) Li, X.; Gao, H.; Murphy, C. J.; Caswell, K. K. *Nano Lett.* **2003**, *3*, 1495–1498.

(52) Greenwood, N. N.; Earnshaw, A. *Chemistry of the Elements*, 2nd ed.; Butterworth-Heinemann: Oxford, U.K., 1997.

(53) Jana, N. R.; Gearheart, L.; Obare, S. O.; Murphy, C. J. *Langmuir* **2002**, *18*, 922–927.

are evenly spaced by the size of a streptavidin molecule (~5 nm), as observed by TEM. This overwhelming preference for end-to-end nanorod assembly is attributed to greater accessibility of the gold surface at the ends of the nanorods by thiol modifiers, relative to the sides of the rods protected by a more densely packed bilayer of CTAB.^{23,40}

More recently, Tan et al.^{40g} produced the same end-to-end assemblies of shorter gold nanorods using different biological linkages, IgG and anti-IgG, characterized by TEM images. This highlights the biorecognition capabilities of modified gold nanorods. In addition to biologically aligned nanorods, Kamat et al.^{40a} has prepared aligned nanorods based on hydrogen bonding. In these experiments, gold nanorods in acetonitrile/water solutions, with surfactants that are presumably on the sides of the nanorods, are modified with acid-terminated thiols. In addition to the observed end-to-end assembly of nanorods in TEM images, absorption spectra of nanorods in solution also show end-to-end alignment, indicated by the red shift of the longitudinal plasmon band due to longitudinal plasmon coupling between hydrogen-bonded nanorods.^{40a}

An alternative approach to using chemical self-assembly to control the nanorod orientation is to use physical means of aligning nanorods. Such physical approaches include alignment of nanorods with electric fields⁵⁴ or stretching of bulk polymers containing nanorods to align them along the stretch direction.^{55–57} Nanorod orientation is typically characterized using polarized absorption spectroscopy. By polarization of incident radiation parallel to the direction of the electric field or the stretch direction, only longitudinal plasmon absorption is observed for aligned gold nanorods.^{40,55,56} Conversely, only transverse plasmon absorption is observed for polarized incident light orthogonal to the aligned nanorods.^{40,55,56} Recently, our laboratory reported using dark-field optical microscopy and atomic force microscopy (AFM) to determine the nanorod orientation in stretched bulk poly(vinyl alcohol) (PVA) and at the surface of PVA.⁵⁶

An additional method for physically aligning 1-D metal nanomaterials would be to align them into grooves or channels on substrates. This has been demonstrated for depositing liquid crystals into grooves on a substrate created by rubbing of the substrate in one direction.⁵⁷ This approach could be extended to assembly of nanorods or nanowires on substrates.

V.B. Ordered Arrays of Spherical Nanoparticles To Make Lines. Many forms of lithography, in which a bulk material is carved up, or stamped upon, to make ordered arrays of nanoscale materials, have been developed.^{19b}

Examples of the assembly of metal nanoparticles, or even metal atoms, in lines are emerging. In separate reports, Atwater et al.^{16a} and Zhang et al.^{16d} have used electron beam lithography to generate arrays of spherical gold nanoparticles in lines on planar substrates. Recently, Mann and co-workers^{16c} have used self-assembly to prepare 1-D chains of gold nanoparticles modified with 2-mercaptoethanol. In all of these examples, the optical properties of the 1-D nanoparticle arrays are significantly different from those of individual spherical particles.

Template methods have also been used to make ordered, wirelike arrays of spherical metal nanoparticles. Matsui and co-workers have used peptide-functionalized heptane dicarboxylate nanowires as templates onto which metal nanoparticles of gold, silver, nickel, and copper can be deposited.⁵⁸ In all of these experiments, bis(*N*- α -amidoglycylglycine)-1,7-heptane dicarboxylate is self-assembled into nanotubes followed by functionalization with peptides to bind metal nanoparticles and act as templates to form metal nanowires. For example, to make gold nanowires by this template approach, heptane dicarboxylate nanotubes were functionalized with histidine-rich peptides known to form metal complexes and to mineralize gold.⁵⁸ Resulting gold and silver nanowires have optical properties comparable to those prepared by colloidal synthetic routes.

VI. Applications of 1-D Metal Nanomaterials

Information technology and nanomaterials overlap in a relatively new field, plasmonics.⁵⁹ Atwater and co-workers have developed nanoparticle waveguides that operate well below the optical diffraction limit, $\lambda/2$, down to $\lambda/20$.^{16a,b} In these systems, arrays of nanoparticles with uniform spaces are assembled in a line on a 2-D substrate by electron beam lithography or by manipulation of nanoparticles using AFM. Incident radiation on one nanoparticle gives rise to plasmon oscillation, which can induce plasmon oscillations to neighboring nanoparticles that are sufficiently close. Then, light coupled through nanoparticle plasmons can propagate along the array, around corners, and through T junctions.

No reports exist that discuss 1-D metals as catalysts, but there is evidence that the nanoparticle shape is important. Recently, El-Sayed reported the use of platinum tetrapod-shaped nanoparticles to catalyze the Suzuki cross-coupling reaction.⁶⁰ While spherical platinum nanoparticles do not catalyze this reaction, tetrapod-shaped nanoparticles do act as a catalyst and undergo a shape change from tetrapods to spheres during these reactions. This suggests that the ends of the tetrapods are significantly more reactive than the core. It would be interesting to see if analogous anisotropic

(54) van der Zande, B. M. I.; Koper, G. J. M.; Lekkerkerker, H. N. W. *J. Phys. Chem.* **1999**, *103*, 5754–5760.

(55) (a) Al-Rawashdeh, N. A. F.; Sandrock, M. L.; Seugling, C. J.; Foss, C. A. *J. Phys. Chem. B* **1998**, *102*, 361–371. (b) van der Zande, B. M. I.; Pages, L.; Hikmet, R. A. M.; van Bladderden, A. *J. Phys. Chem. B* **1999**, *103*, 5761–5767. (c) Pérez-Juste, J.; Rodríguez-González, B.; Mulvaney, P.; Liz-Marzán, L. M. *Adv. Funct. Mater.* **2005**, *15*, 1065–1071.

(56) Murphy, C. J.; Orendorff, C. J. *Adv. Mater.* **2005**, *17*, 2173–2177.

(57) Varghese, S.; Narayanankutty, S.; Bastiaansen, C. W. M.; Crawford, G. P.; Broer, D. J. *Adv. Mater.* **2004**, *16*, 1600–1605.

(58) (a) Djalali, R.; Chen, Y.; Matsui, H. *J. Am. Chem. Soc.* **2002**, *124*, 13660–13661. (b) Djalali, R.; Chen, Y.; Matsui, H. *J. Am. Chem. Soc.* **2003**, *125*, 5873–5879. (c) Yu, L.; Banerjee, I. A.; Matsui, H. *J. Am. Chem. Soc.* **2003**, *125*, 14837–14840. (d) Yu, L.; Banerjee, I. A.; Shima, M.; Rajan, K.; Matsui, H. *Adv. Mater.* **2004**, *16*, 709–712. (e) Banerjee, I. A.; Yu, L.; Matsui, H. *Proc. Natl. Acad. Sci. U.S.A.* **2003**, *100*, 14678–14682.

(59) Atwater, H. A.; Maier, S.; Polman, A.; Dionne, J. A.; Sweatlock, L. *MRS Bull.* **2005**, *30*, 385–389.

(60) Narayanan, R.; El-Sayed, M. A. *Langmuir* **2005**, *21*, 2027–2033.

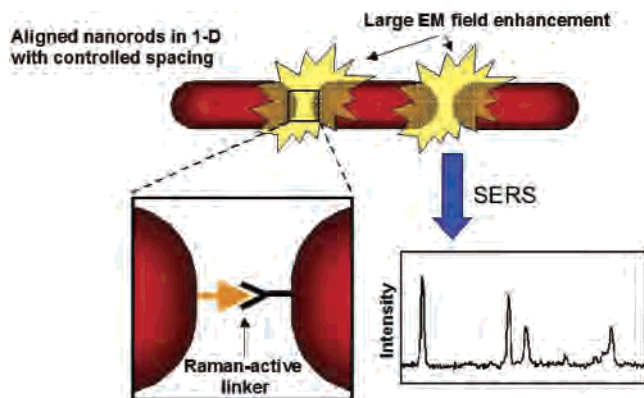


Figure 8. Cartoon of aligned nanorods in one dimension where longitudinal plasmon coupling increases the EM field at the ends of the nanorods. Using a Raman-active linker to align the nanorods, the Raman cross section of that molecule could be significantly enhanced in this geometry.

reactivity is observed for 1-D metal nanorods or nanowires used as catalysts.

Chemical sensing and spectroscopy with 1-D metal nanostructures is a rapidly growing area. This is especially true in the field of SERS, where the Raman scattering cross section of a molecule is significantly enhanced when that molecule is adsorbed to the surface of gold or silver that is rough on the nanoscale. It is generally agreed that large EM field enhancement near the nanoparticle surface, from metal nanoparticle LSPR, is primarily responsible for SERS and other closely related techniques.⁶¹ Although the SERS phenomenon has been around for nearly 40 years, there has been resurgence in the field in recent years using colloidal or lithographically prepared nanoparticle substrates. While the Raman scattering cross section of a molecule at the surface of an isolated nanoparticle is increased by 4–6 orders of magnitude, placing a molecule between two nanoparticles increases its effective scattering cross section by 10–12 orders of magnitude as a result of plasmon coupling and larger EM field enhancement. This colossal increase in the effective scattering cross section leads to single-molecule SERS reported by Kneipp et al.⁶²

Theoretical work by Schatz et al.⁴⁴ has calculated the greatest EM field enhancement at the ends of isolated nanorods and nanowires compared to other nanoparticle shapes, making them attractive substrates for SERS and surface-enhanced fluorescence (SEF). Then, end-to-end-aligned nanorods in one dimension, as described above, present an interesting geometry for SERS, where large EM fields at the ends of neighboring nanorods can be coupled; this is represented by a cartoon in Figure 8. There have been several reports for SERS on silver nanowires and on gold nanorods.^{23c,63} For example, Moskovits and co-workers recently studied polarization-dependent SERS on silver nanowire bundles or rafts.⁶⁴ They observed greater EM

enhancement with incident light polarized across the nanowire bundle (across the short axes of many wires) than with incident light polarized along the length of a bundle (along the long axis of only a few wires). Greater EM enhancement is attributed to nanowire plasmon coupling or SERS “hot spots” for molecules adsorbed in the fractal space between wires. Recently, we have studied SERS on gold and silver nanorods of different aspect ratios in aqueous solution.⁶⁵ For nanorods with longitudinal plasmon bands in resonance with the excitation source, a 10^2 increase in EM enhancement was observed for both gold and silver nanorods than for nanorods with plasmon bands in the off-resonance condition.

While SEF has been reported on metal nanoparticle substrates,⁶⁶ it has not been extended to 1-D metal nanorods or nanowires. If a fluorophore and the metal nanoparticle surface are separated by ~ 10 nm or more, fluorescence is enhanced by up to 2 orders of magnitude by the localized electric field and the intrinsic decay of the fluorophore. Because large electric field enhancements are observed at the ends of nanorods and nanowires, it seems that designing SEF experiments localized at the ends of nanorods or nanowires would be of interest.

VII. Key Challenges

Given all of the promise of colloidal 1-D metal nanostructures, what are the major challenges? We identify several. First of all, although there has been great progress in shape control at the nanoscale, yields of materials are still relatively low and reports of gram-scale syntheses are rare. Second, rational organization of nanocrystals into well-defined arrays is still challenging to actually perform in the laboratory, let alone on the scale of mass production. Given that these two conditions are met, then many applications (catalysis, chemical sensing via surface-enhanced spectroscopies, plasmonics, etc.) can be further developed to yield exciting new technologies that can benefit such diverse areas as chemical manufacturing, medical diagnostics, information technology, and national security.

Acknowledgment. We thank Tan Li for assistance in the preparation of this Forum Article and former members of the Murphy laboratory for their hard work. We thank the National Science Foundation and the University of South Carolina for funding and Professor Hans-Conrad zur Loye and his group for assistance with the magnetic measurements.

IC0519382

- (61) (a) Johansson, P.; Xu, H.; Kall, M. *Phys. Rev. B* **2005**, *72*, 035427/1–035427/17. (b) Xu, H.; Wang, X.-H.; Persson, M. P.; Xu, H. Q.; Kall, M.; Johansson, P. *Phys. Rev. Lett.* **2004**, *93*, 243002/1–243002/4.
- (62) Kneipp, K.; Wang, Y.; Kneipp, H.; Perelman, L. T.; Itzkan, I.; Dasari, R. R.; Feld, M. S. *Phys. Rev. Lett.* **1997**, *78*, 1667–1670.

- (63) (a) Tao, A.; Kim, F.; Hess, C.; Goldberger, J.; He, R.; Sun, Y.; Xia, Y.; Yang, P. *Nano Lett.* **2003**, *3*, 1229–1233. (b) Aroca, R. F.; Goulet, P. J. G.; dos Santos, D. S.; Alvarez-Puebla, R. A.; Oliverira, O. N. *Anal. Chem.* **2005**, *77*, 378–382. (c) Nikoobakht, B.; El-Sayed, M. A. *J. Phys. Chem. A* **2003**, *107*, 3372–3378. (d) Orendorff, C. J.; Gole, A.; Sau, T. K.; Murphy, C. J. *Anal. Chem.* **2005**, *77*, 3261–3266.
- (64) Jeong, D. H.; Zhang, Y. X.; Moskovits, M. *J. Phys. Chem. B* **2004**, *108*, 12724–12728.
- (65) Orendorff, C. J.; Gearheart, L.; Jana, N. R.; Murphy, C. J. *Phys. Chem. Chem. Phys.* **2006**, *8*, 165–170.
- (66) (a) Parfenov, A.; Gryczynski, I.; Malicka, J.; Geddes, C. D.; Lackowicz, J. R. *J. Phys. Chem. B* **2003**, *107*, 8829–8833. (b) Lackowicz, J. R.; Geddes, C. D.; Gryczynski, I.; Malicka, J.; Gryczynski, Z.; Aslan, K.; Lukomska, J.; Matveeva, E.; Zhang, J.; Badugu, R.; Huang, J. J. *Fluoresc.* **2004**, *14*, 425–441.